

Modeling and analysis of boost converter in small-signals applied to the wind energy conversion system using Matlab/Simulink

N. Nisso ^{1*}, D. Raïdandi ^{1,2}, N. Djongyang ¹ and F.D. Menga ^{1,3}

¹ Department of Renewable Energy, National Advanced School of Engineering of Maroua University of Maroua, Cameroon

² Department of Mechanical Engineering, National Advanced School of Engineering of Yaoundé, University of Yaoundé I, Cameroon

³ National Committee for Technology Development
Ministry of Scientific Research and Innovation, Yaoundé, Cameroon

(reçu le 21 Novembre 2018 - accepté le 20 Décembre 2018)

Abstract - *The problem of stabilizing a boost converter in small-signal situations using linear control laws is derived by the means of oriented circuit procedure. After establishing a small-signal circuit model for the boost regulator including state-feedback, conditions for the stability of circuit are studied. Thereafter, a linear analysis is performed in order to design the desired dynamics and robust behavior of the boost converter. The linear analysis assumed shows that only a state feedback gain matrix is necessary, provided that the coordinates of the equilibrium point are known. This operation is done by using the root locus method to choose the eigenvalue of this gain vector. It aims at presenting how boost converter averaged behavior can be tailored by means of feedback control structures. Various control structures with different design methods have become classical in control systems theory with a similar degree of efficiency. It is generally assumed that the obtained control input is applied to boost converter by using pulse-width modulation. Performance of the proposed pole placement method is evaluated by Simpower/Matlab simulation at the equilibrium operating points chosen. To verify a feasibility of the proposed method, set parameters of system is implemented. The control scheme is verified through Matlab simulation, which is present to verify the performance of proposed method and simulation results validate the analytical predictions. The circuit studied is an element of the wind energy conversion system (WECS).*

Résumé - *La stabilisation de tension à l'aide d'un convertisseur Boost par l'utilisation des lois de commande linéaire est déduite par une procédure du circuit orienté. Après avoir établi le modèle équivalent du circuit Boost et du retour d'état, les conditions de stabilité du circuit sont élaborées. Ensuite, une analyse linéaire est effectuée afin de se pencher sur le comportement dynamique et robuste du circuit. L'analyse linéaire montre que seule une matrice gain de retour d'état est nécessaire, à condition que les coordonnées du point d'équilibre soient connues. Pour cela la méthode des lieux de racine est appliquée pour conduire au choix de la valeur propre de ce vecteur gain. L'objectif est de montrer comment le comportement moyenné du convertisseur Boost peut être adapté au moyen de structures de contrôle à rétroaction. Diverses structures de contrôle avec différentes méthodes de conception sont devenues classiques dans l'étude des systèmes de contrôle avec un degré d'efficacité similaire. Nous admettons que l'entrée de commande obtenue est appliquée au convertisseur Boost en utilisant une modulation de largeur d'impulsion (MLI). Les performances de la méthode de placement de pôles proposée sont évaluées par simulation aux points de fonctionnement d'équilibre choisis. Pour vérifier la faisabilité de la méthode proposée, un ensemble de paramètres définis du système est implémenté. Le schéma de contrôle est vérifié à l'aide d'une simulation sous Matlab/SimPowerSystems, pour confirmer les performances de la méthode proposée et de valider les résultats des*

* nnicodem2000@yahoo.fr

prévisions analytiques. Le circuit étudié est un élément du système de conversion de l'énergie éolienne (SCEE).

Keywords: Pole placement - Boost converters - Small-signal stability - Gain vector - WECS.

1. INTRODUCTION

The basic operation of the feedback loop [1, 2] using boost converter [3, 4] consists to compare the output variable with a reference input to generate an error signal, which, after being appropriately filtered and amplified, results in a continuous control signal. This signal is eventually transformed by means of PWM defining the switch duty cycle.

The main difficulties in the analysis of boost converter are due to the nonlinear nature of system. If there are no constraints on amplitude or frequency of perturbations in input voltage, load or external reference, we can always simulate the state equations describing the boost converter dynamic behavior, but this simulation requires a high computation time and does not provide enough information to synthesize the control loop.

Finding the exact analytical solution of the state equations is also possible, although the resulting formulation cannot be easily applied. These obstacles have oriented this work in this field toward establishing, with some assumptions, boost converter models that can be analytically exploited or specifically oriented to numerical simulation with small computation times.

The boost converter dynamic behavior [5] can be described by means of linear model if the amplitude of the disturbance is significantly smaller than the steady-state value of the state vector.

Linear continuous models are very widespread among designers because classical linear-feedback theory can be easily used for stability analysis and design of feedback compensation system. However, it is well known that the validity of linear models is constrained to a small area around the steady-state operation point.

These disadvantages have led some authors to explore nonlinear techniques in order to undertake the control loop synthesis. The use of these techniques is justified by the bilinear nature of the boost converter dynamic behavior and by the limitation of the duty cycle to remain in the interval $[0, 1]$.

The utilization of linearized control to guarantee global stability in the boost converter was proposed in using Lyapunov functions [6]. Similarly, global stability is ensured in [7] through a Lyapunov-based control design which provides the feedback gain matrix through an iterative procedure.

Limits between stable and unstable areas for different values of parameters are studied in [8] through numerical simulation. A modified small-signal model is used in [9] to predict the large signal behavior boost converter operating under pulsed load.

The stability graphs are developed in [10] to estimate the values of input voltage and load resistance leading to a stable design under large-signal operation. The boundaries of the feedback gains that define the region inside which global stability is ensured.

In [11] the boundaries of the feedback gains that define the region inside which global stability is acquired using a nonlinear discrete model of the boost converter. A control technique is developed based on the expression of the saltation matrix to control nonlinear behaviors in a boost converter [12]. The boost converter in [13] has been used to achieve the maximum power output of the wind energy by the segmented regulation by applying the two-voltage stage topology. The research in [14] reveals the robustness

and the dynamical performances of a boost converter applied on electric vehicle by using the fuzzy sliding mode technique.

The regulation of the output voltage of a boost converter when the duty cycle is subjected to the saturation has been addressed in [15]. The controller designed exploited losses due to parasitic resistances of passive components. The foraging behavior of a colony of honey bees is meticulously studied and therefore an optimization algorithm is designed to control a boost converter [16]. A small signal model of a boost converter to evaluate the accuracy of redesign approaches and direct digital designs, in term of output voltage transients is treated in [17].

Contrary to our analysis, a cascade output voltage control scheme without the use of any boost converter parameter is found in [18]. Some of the papers propose nonlinear control laws of boost converter as fuzzy-PID control [19]. Some papers deal with pole compensation to synthesize the PI controllers [20] but not to study the regulation of the output of boost converter.

The papers cited previously do not use the technique of pole placement not only to study the stability of the boost converters but also and especially for the regulation of the output voltage. The aim of this paper is to present a new method based on a pole placement, to analyze the stability of the boost converter in small signals case. Knowing that the maximum output voltage, it is required that the output voltage tracks – with zero steady-state error – the desired reference.

Global stability is analyzed by studying the small-signal linearized model of the boost converter, while meeting a set of imposed performance requirements. Pole placement method is useful for conveniently place the closed-loop eigenvalues when full-state feedback information is available. The root locus method will provide a powerful tool for deriving controllers that ensure robust closed-loop behavior [21].

In Section 2, the equivalent device of a boost converter is reviewed. The small-signal stability by means of linear feedback is analyzed. The boost converter model, based on physical description by differential equations and on the classical assumption of perfect switches, is described.

This model succeeds in capturing the time-varying nature of the device; it will be used directly for simulation purpose by employing a pole placement control laws design.

The state-space averaged model for small-signal behavior of the boost converter is studied and its limitations are assessed all this in section 3. Numerical simulation results are shown in Section 4. Finally, conclusion and references are presented in section 5 and section 6 respectively.

2. MODELING OF LINEAR BOOST CONVERTER

2.1 Basic modeling

Figure 1 shows the boost converter analyzed in this paper, that is assumed to operate in continuous conduction mode [22]. V_c is the output voltage, E is the line voltage and i_s is the load disturbance. The output voltage must be kept at a known value V_{Cref} . The boost converter is connected to a load modeled as a linear resistor R .

The capacitance of the capacitor and the inductance of the inductor are represented, respectively, by C and L . Their equivalent series resistances, r_C and r_L , are considered sufficiently small to be not considered. Therefore, the measurable states of the boost converter are the inductor current i_L and the capacitor voltage v_C [23].

The boost converter can take two configurations, as shown in figure 2: cases (a) and (b) correspond to switch SW being turned ON and turned OFF respectively.

The boost converter is driven by a binary signal $u(t)$, called the switching function [24]. A modulating signal have to be compared with a sawtooth voltage waveform signal to generate the gate-driving signals, as shown in figure 3.

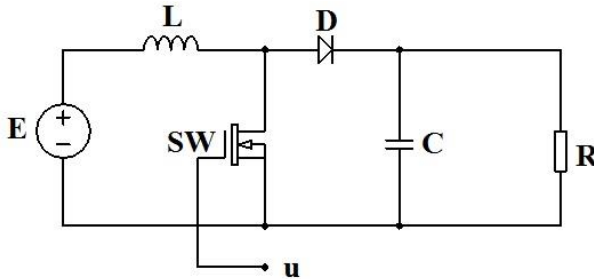


Fig. 1: Boost converter topology

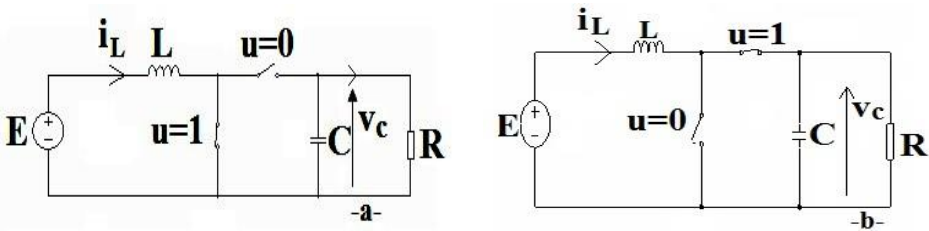


Fig. 2: Boost converter configuration (a) switch turned ON (b) switch turned OFF

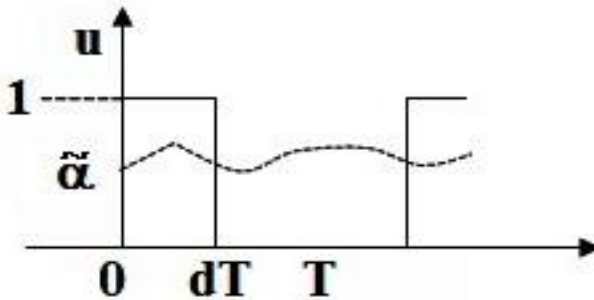


Fig. 3: Waveforms of the PWM process

Let us consider that $u(t)$ is periodic, with T considered as switching period and α being duty ratio:

$$u(t) = \begin{cases} 1, & 0 \leq t < \alpha T \\ 0, & \alpha T \leq t < T \end{cases} \quad u(t - T) = u(t)$$

The inductor current I_L and the capacitor voltage V_C are the state variables. The state equations [25] corresponding to the two circuit schemes are listed below:

$$u = 1 : \begin{cases} \dot{I}_L = \frac{E}{L} \\ \dot{V}_C = -\frac{V_C}{RC} \end{cases} \quad u = 0 : \begin{cases} \dot{I}_L = \frac{E}{L} - \frac{V_C}{L} \\ \dot{V}_C = \frac{I_L}{C} - \frac{V_C}{RC} \end{cases} \quad (1)$$

Equations from (1) can be reduced into a single form by multiplying the equations for the ON system by u and the equations for the OFF systems by $1-u$.

$$\begin{cases} \dot{I}_L = \frac{E}{L}u + \frac{E-V_C}{L}(1-u) \\ \dot{V}_C = -\frac{V_C}{RC}u + \left(\frac{I_L}{C} - \frac{V_C}{RC}\right)(1-u) \end{cases} \quad (2)$$

From the previous equation, we can derive

$$\begin{cases} \dot{I}_L = -(1-u)\frac{V_C}{L} + \frac{E}{L} \\ \dot{V}_C = (1-u)\frac{I_L}{C} - \frac{V_C}{RC} \end{cases} \quad (3)$$

Equation (3) make possible the bilinear form [26]:

$$\begin{bmatrix} \dot{I}_L \\ \dot{V}_C \end{bmatrix} = \begin{bmatrix} 0 & -\frac{1}{L} \\ \frac{1}{C} & -\frac{1}{RC} \end{bmatrix} \begin{bmatrix} I_L \\ V_C \end{bmatrix} + \begin{bmatrix} 0 & \frac{1}{L} \\ -\frac{1}{C} & 0 \end{bmatrix} \begin{bmatrix} I_L \\ V_C \end{bmatrix} u + \begin{bmatrix} \frac{E}{L} \\ 0 \end{bmatrix} \quad (4)$$

2.2 Small-Signal modeling of the boost converter

With the purpose of perform the small-signal analysis of the boost converter [27] the notations for the averages of the state variables are denoted in the following way:

$$i_C = I_C \quad v_C = V_C$$

From (3), the small-signal averaged model is obtained by:

$$\begin{cases} \dot{i}_L = -(1-u)\frac{v_C}{L} + \frac{E}{L} \\ \dot{v}_C = (1-u)\frac{i_L}{C} - \frac{v_C}{RC} \end{cases} \quad (5)$$

By cancelling the derivatives in (5) one obtains the steady-state input-output characteristic [28]. It is the locus of the system's equilibrium points, denoted with the subscript e .

$$\begin{cases} i_{Le} = \frac{E_e}{(1-u_e)^2 R} \\ v_{Ce} = \frac{E_e}{(1-u_e)} \end{cases} \quad (6)$$

Equation (6) gives the static behavior of the boost converter. The derivation of the large-signal model of the boost converter will be performed around the equilibrium point with the purpose of to extract the small-signal model. " \sim " denotes the small variations around the equilibrium point. All variables in the system may be written around the equilibrium point of the following way [29]:

$$\begin{cases} \alpha = \alpha_e + \tilde{\alpha} \\ u = u_e + \tilde{u} \\ i_L = i_{Le} + \tilde{i}_L \\ v_C = v_{Ce} + \tilde{v}_C \\ E = E_e + \tilde{E} \end{cases} \quad (7)$$

The state-space model can be easily expressed as:

$$\begin{cases} L \dot{\tilde{i}}_L = (E_e + \tilde{E}) - (1 - u_e - \tilde{u})(v_{Ce} + \tilde{v}_C) \\ C \dot{\tilde{v}}_C = (i_{Le} + \tilde{i}_L)(1 - u_e - \tilde{u}) - \frac{(v_{Ce} + \tilde{v}_C)}{R} \end{cases} \quad (8)$$

We resort to the Taylor series development limited to the first order around the equilibrium operating points chosen. One obtains:

$$\begin{cases} L \dot{\tilde{i}}_L = E_e + \tilde{E} - (1 - u_e)v_{Ce} - (1 - u_e)\tilde{v}_C + v_{Ce}\tilde{u} + \tilde{v}_C\tilde{u} \\ C \dot{\tilde{v}}_C = (1 - u_e)i_{Le} + (1 - u_e)\tilde{i}_L - \frac{\tilde{v}_C}{R} - i_{Le}\tilde{u} - \frac{v_{Ce}}{R} - \tilde{i}_L\tilde{u} \end{cases} \quad (9)$$

Using relations (6) in the system of (9) and neglecting small variations, therefore we find easily the small-signal average model of the boost converter:

$$\begin{cases} L \dot{\tilde{i}}_L = -(1 - u_e)\tilde{v}_C + v_{Ce}\tilde{u} + \tilde{E} \\ C \dot{\tilde{v}}_C = (1 - u_e)\tilde{i}_L - \frac{\tilde{v}_C}{R} - i_{Le}\tilde{u} \end{cases} \quad (10)$$

$$\begin{cases} \dot{\tilde{i}}_L = -\frac{u'_e}{L}\tilde{v}_C + \frac{v_{Ce}}{L}\tilde{u} + \tilde{E} \\ \dot{\tilde{v}}_C = \frac{u'_e}{C}\tilde{i}_L - \frac{\tilde{v}_C}{R_e C} - \frac{i_{Le}}{C}\tilde{u} \end{cases} \quad (11)$$

The last equation traduces the linearity of boost converter. Therefore, it will be easy to control. From (11), we can also obtain the plant original circuit to study the stabilization of system.

The term \tilde{E} is the variation of the supply circuit. It can be due to intermittent nature of wind [30]. This disturbance must to be taken account conveniently. In the aim to design the control strategy, first assume that the perturbations in the output current is null.

Equation (11) can be rewritten as follows:

$$\begin{cases} \dot{x} = Ax + B\alpha \\ y = Cx \end{cases} \quad (12)$$

Where x and y being the state vector and output vector, respectively, and A , B , and C the matrices of the averaged state space model in small signal with their values given by:

$$A = \begin{bmatrix} 0 & -\frac{\alpha'_e}{L} \\ \frac{\alpha'_e}{C} & -\frac{1}{R_e C} \end{bmatrix} \quad B = \begin{bmatrix} \frac{v_{Ce}}{L} \\ -\frac{i_{Le}}{C} \end{bmatrix} \quad C = [0 \quad 1] \quad (13)$$

3. LINEAR CONTROL LAWS FOR SMALL-SIGNAL

The averaged dynamics of the boost converter are unsuitable for control purposes and cannot be properly compensated by a single control loop [31]. A useful modelling that has become classic in systems theory is to separately compensate the boost converter dynamics by a second state feedback loop and to steer the system output towards the desired set-point by a primary control loop.

For that reason, the state feedback loop arrange differently the systems pole-zero map in a convenient model such as the inner closed loop has some prerequisite features: high natural frequency, high damping factor. This allows the using of a simple controller, an integrator, in the outer loop for purposes of output variable regulation or tracking [32].

Assumptions

One specify some simplifying assumptions, sufficiently accurate so as not to influence the validity of the models to be implemented [33]:

- Diode and transistor taken as switches are considered perfect in the sense that during the time conduction, the resistance value is zero and when the switch is turned off, the resistance value is infinite. Also, the switching time is infinitely short;
- DC voltage sources are considered perfect;
- Resistor, capacitor and inductor considered, as passive components are linear, time invariant, and frequency independent;

All state variables are available for measure. Also, it is assumed that the small ripple condition is fulfilled and the boost converter operates in CCM. Output voltage control is achieved by means of the simple but very powerful idea of feedback loop and is based on the boost converter averaged linear model. This allows closing the system loop and presents a way to conveniently change its static and dynamic properties.

The integral control used to ensure zero steady state error within a reasonable time for a highly undamped plant quickly results in stability loss. This will be easily possible by using the root locus method [34]. It is imposed first some convenient dynamic by using the pole placement method [35]. The figure 4 shows the general structure of controlled circuit.

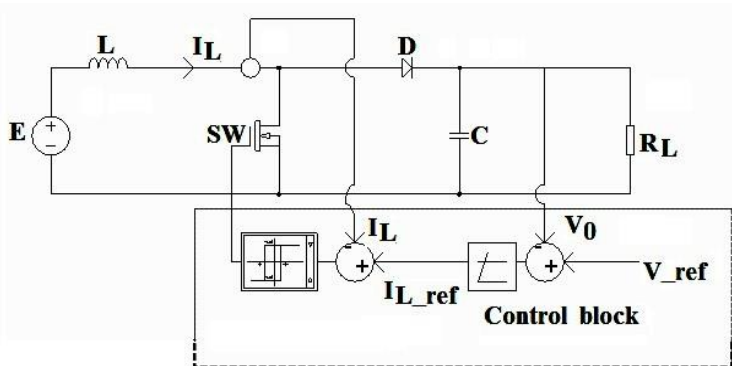


Fig. 4: General structure of controlled circuit

Accordingly, the desired poles can be arranged by a full state feedback gain vector, denoted by K in figure 5. To facilitate the design further, it will be imposed a pair of complex-conjugated poles. The second order-closed loop dynamic may subsequently be

adjusted via the root locus technique by choosing a convenient closed-loop pole placement as the integral gain vector \mathbf{K} varies.

The plant of boost converter is described by a small signal averaged linearized model in (12). The state includes measurable currents and voltages and α is the duty ratio.

The inner plant having variable v as input, variable y as output and vector x as state is described by the state matrix $A_i = A - \mathbf{BK}$, the input matrix \mathbf{B} and the output matrix \mathbf{C} . The desired set of eigenvalues on the closed-loop state matrix A_i is fixed and the necessary feedback gain \mathbf{K} is obtained. The resulting transfer function is therefore obtained as:

$$H_i(s) = C (sI_2 - A_i)^{-1} B \tag{14}$$

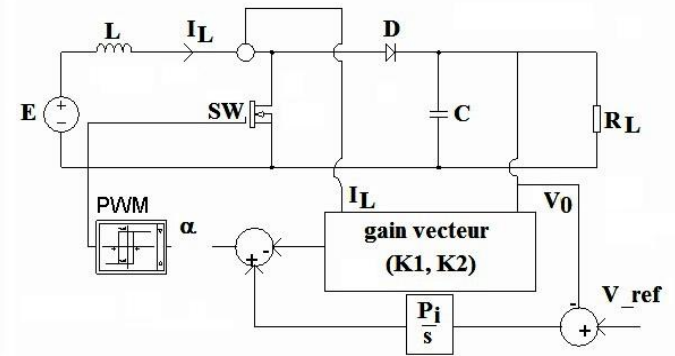


Fig. 5: Output regulation structure using state-feedback-based inner loop

Where I_2 is the identity matrix of the same dimension as the state matrix A . It appears that the inner plants' dynamic properties can effectively be adjusted by imposing the eigenvalues of matrix A_i , and this can be effectively done by choosing a convenient gain vector, \mathbf{K} . Due to this inner state feedback, the plant's original poles are moved to new positions at higher natural frequencies and higher damping [18].

The boost converter has a two-state converter, therefore the gain vector $\mathbf{K} = [k_1 \quad k_2]$ ensuring the closed loop poles are placed as specified by a vector $\mathbf{P} = [p_1 \quad p_2]^T$.

To evaluate feedback gains k_i , the eigenvalues of $A - \mathbf{BK}$ can be assigned by a closed loop pole-placement. One simple approach to do this is to calculate analytically the characteristic polynomial of $A - \mathbf{BK}$ and identify its coefficients using another polynomial that has the desired dominant poles p_i as its roots:

$$\det(sI_2 - A_i) = (s - p_1)(s - p_2) \tag{15}$$

We have to be imposed a pair of complex-conjugated poles, therefore the following relations hold:

$$\begin{cases} -(p_1 + p_2) = 2\xi_n \omega_n \\ p_1 p_2 = \omega_n^2 \end{cases} \tag{16}$$

In (15) ω_n being the desired closed-loop band width and ξ_n being the desired closed-loop damping coefficient [36].

One can use the Matlab command for finding the state feedback coefficients by Ackerman formula as following:

$$K = \text{acker}(A, B, P) \tag{17}$$

We find the closed-loop transfer function from the equation (14) and (17).

$$H_i(s) = \frac{sb_2 + b_2(b_1k_1 - a_{11}) + b_1(a_{21} - b_2k_1)}{s^2 + (b_1k_1 + b_2k_2 - a_{11} - a_{22})s + a_{11}a_{22} - a_{12}a_{21} + a_{12}b_2k_1 - a_{22}b_1k_1 + a_{21}b_1k_2 - a_{11}b_2k_2}$$

Where a_{ij} and b_i are the elements of matrix A and B respectively. These coefficients are defined by:

$$a_{11} = 0; a_{12} = -\frac{\alpha'_e}{L}; a_{21} = \frac{\alpha'_e}{C}; a_{22} = -\frac{1}{R_e C}; b_1 = \frac{V_{Ce}}{L}; b_2 = -\frac{i_{Le}}{C} \tag{19}$$

Now let us approach the outer loop, dedicated to outer voltage regulation. The corresponding open loop transfer function is

$$H_{BO}(s) = \frac{P_i}{s} H_i(s) \tag{20}$$

The aim is to choose a sufficiently high value for the integrator gain P_i so as to ensure the required closed-loop bandwidth with convenient damping. We use the root locus method for this operation [37].

4. CONTROL IMPLEMENTATION FOR SMALL SIGNAL STABILITY

The Matlab simulation is carried out as shown in this section and the model circuit is depicted in figure 6. The set of parameters chosen is shown in **Table 1** and these numerical values give good performance. The parameters of **Table 2** were selected using pole placement techniques after linearizing around a typical operating point.

Establishment time and robustness of the transient response are taken in account. In order to choose the value of the gain vector described above by pole placement technique, we analyze the root locus. Note that a linear analysis is performed once that the small signal stability has been guaranteed. The linear analysis does not take into account bilinear terms [38].

Table 1: Signal statistics of output voltage

	Value (V)	Time (s)
Max	27.06	1.85
Min	0.04886	//
Peak to peak	27.2	//
Mean	24.73	//
Median	25	//
RMS	24.79	//

The results are obtained using the previous equations. Figure 7 shows Matlab simulations of the inductor voltage and current waveforms based on the steady state. The Matlab simulation result of controlled voltage is shown in below figure 8.

It appears that our controller achieves better performance and the overshoot is 5.17 %. Figure 9 describes the root locus for system described by (20) and position of poles for different values of controller gain P_i (0, 600, 850).

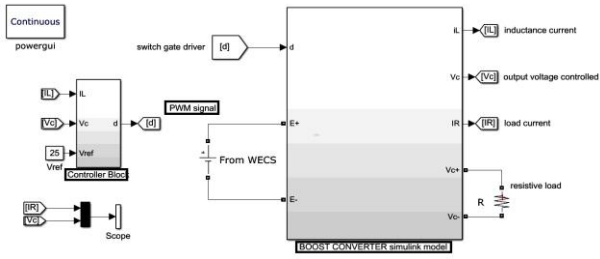


Fig. 6: Boost converter Matlab/Simulink model

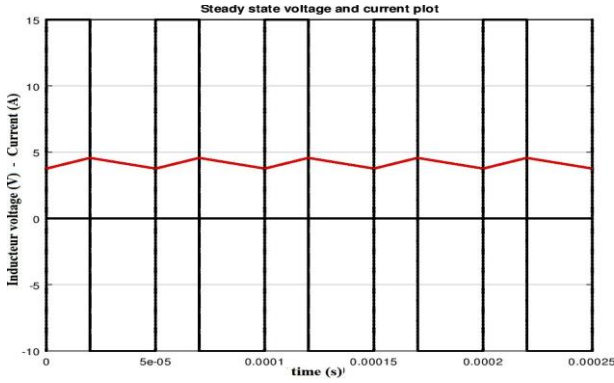


Fig. 7: The waveform of inductor voltage and current of boost converter on the steady state

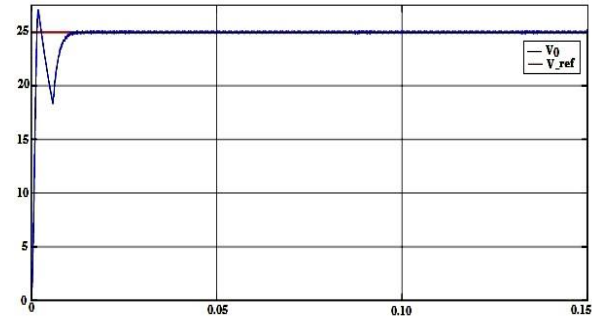


Fig. 8: Matlab simulation result of controlled voltage

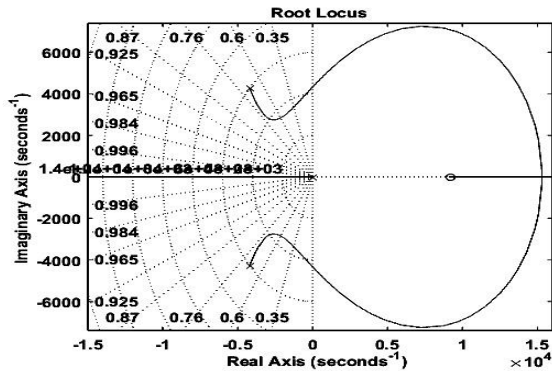


Fig. 9: Root locus for the pole placement

Table 2: Specifications of the boost converter

Parameters	Value	Designation
R	10 Ω	Load resistance
L	0.372 mH	Inductance
C	1000 μF	Capacitance
E	15 V	Input supply voltage
T	50 μS	Switch frequency
α_e	0.4	Duty cycle
i_{Le}	4.1667 A	inductor steady-state current
v_{Ce}	25 V	Desired output voltage

The transfer function (18) is numerically evaluated as

$$H_i(s) = \frac{-4167s + 3.824 \times 10^7}{s^2 + 8400s + 3.596 \times 10^7} \tag{21}$$

The transfer function shows that it is a non-minimum phase system having a zero on the right-half s-plane [39]. The bode plot of the above transfer function as shown in figure 10 reveals that the gain margin (Gm) of the system is negative. The phase margin (Pm) is 75.3° at a frequency of 5040 rad/s. The nyquist diagram in figure 11 shows that the system studied in closed loop is stable.

Table 3: Gain vector parameters

Parameters	Value
K_1	0.2535
K_2	1.1697

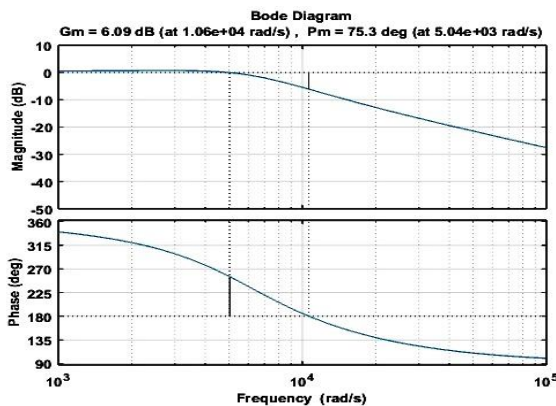


Fig. 10: Bode plot of output to control input transfer function

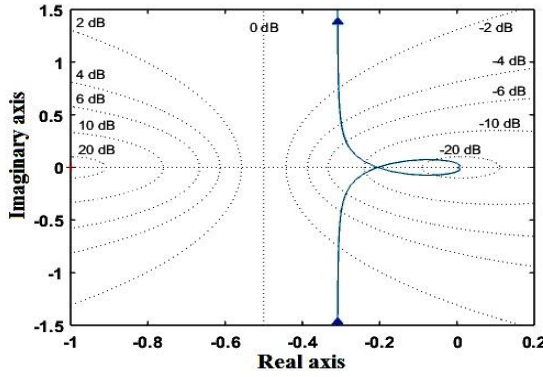


Fig. 11: Nyquist diagram

5. CONCLUSIONS

In this paper, small-signal stability of linear control laws for boost converter have been studied. The circuit model used in this study has been analyzed. This model describes variable relationships, where the energy in the storing passive elements constitutes the perturbation energy with respect to the equilibrium point. The analysis takes into account linear terms.

Once that small-signal stability for the linear control law has been demonstrated, response frequency, root locus and pole placement techniques has been employed to guarantee robustness and good transient response.

Contrary to classical control methods of boost converter, the technique here reported guarantees small-signal stability of the boost converter. In our design, we have first guaranteed small-signal stability of a linearly controlled boost converter by means of a linear analysis. Thereafter, we have designed the feedback loop using pole placement techniques. Observe that linearization constrains in the previous equations have been used in the stability investigation.

Finally, as a possible direction for future research, this methodology can be applied in the buck-boost converter. Also, it can be easily applied to a buck whose dynamics linked to bilinear terms are neglected. Another interesting future research topic is associating pole placement to fuzzy control approach, for the trajectory tracking task in boost converter.

NOMENCLATURE

i_S , Load disturbance, A	R , Load modeled as a linear resistor, Ω
C , Capacitance of the capacitor, F	L , Inductance of the inductor, H
D , Diode	r_C, r_L , Equivalent series resistances, Ω
I_L, \dot{i}_L , Inductor current, A	I_{L-ref} , Reference Inductor current, A
$V_{Cref}, v_C, v_{Ce}, \tilde{v}_C, \tilde{\tilde{v}}_C$, Capacitor voltage, V	SW , Mosfet transistor considered as switch V_O , output voltage, V
V_{ref} , Reference voltage, V	$u(t), u_e, \tilde{u}, u'_e$, Binary signal
$\alpha, \alpha_e, \tilde{\alpha}, \alpha'_e$, Duty ratio	T , Considered as switching period, s
$\dot{i}_{Le}, \tilde{i}_L, \tilde{\tilde{i}}$, Inductor steady-state current, A	E, E_e, \tilde{E} , Input supply voltage, V

x, \dot{x} , State vector	y , Output vector
t , time, s K , Gain vector	A_i, A, B, C , Matrices of the averaged state space model
H_i , Transfer function	I_2 , 2x2 identity matrix
k_i , Feedback gains	$P = [p_1 \ p_2]^T$, Vector with elements
s , Laplace variable	P_i , Integrator gain
ω_n , Desired closed-loop bandwidth, rad/s	ζ_n , Desired closed-loop damping coef.
a_{ij}, b_i , elements of matrix A an B respec.	H_{BO} , Open loop transfer function
Gm , Gain margin, dB	Pm , Phase margin, °C

REFERENCES

- [1] S. Nanda, M. Sengupta, and A. Sengupta, 'Modelling, Simulation, Fabrication, Experiments and Real-Time Linear State Variable Feedback Control of Cuk Converter using Pole Placement Technique', Journal of the Institution of Engineers, Séries B, Vol. 95, N°1, pp. 55 - 62, 2014.
- [2] C.-C. Hua, H.-C. Chiang, and C.-W. Chuang, 'Small signal analysis of a new boost converter based on Sheppard-Taylor topology', Journal of the Chinese Institute of Engineers, Vol. 37, N°3, pp. 346 - 357, 2014.
- [3] M. Sai Krishna Reddy, C. Kalyani, M. Uthra, and D. Elangovan, 'A small signal analysis of DC-DC boost converter', Indian Journal of Science and Technology, Vol. 8, S2, pp. 1 - 6, 2015.
- [4] R. Kot, M. Rolak, and M. Malinowski, 'Comparison of maximum peak power tracking algorithms for a small wind turbine', Mathematics and Computers in Simulation, Vol. 91, C, pp. 29-40, 2013.
- [5] M.H. Rashid, '*Power electronics handbook: devices, circuits and applications*', Third Edit. Elsevier Inc., 2011.
- [6] M. Chadli, P. Borne, and B. Dubuisson, 'Multiple Models Approach in Automation: Takagi-Sugeno Fuzzy Systems', ISTE Ltd, 2013.
- [7] S.R. Sanders, 'Nonlinear control of switching power converters', Massachusetts Institute of Technology, 1989.
- [8] J. Channegowda, B. Saritha, H.R. Chola, and G. Narayanan, 'Comparative evaluation of switching and average models of a DC-DC boost converter for real-time simulation', in IEEE Conecct, 2014, IEEE International Conference on Electronics, Computing and Communication Technologies, pp. 1 - 6, 2014.
- [9] J. Arau and Q. Jimenez, 'Improving large signal analysis in DC/DC converters with a modified small signal model', PESC'92 Rec. 23rd Annual IEEE Power Electronics Specialists Conference, 1992.
- [10] F. Guinjoan, J. Calvente, A. Poveda, and L. Martínez, 'Large-signal modeling and simulation of switching dc-dc converters', IEEE Transactions on Power Electronics, Vol. 12, N°3, pp. 485 - 494, 1997.

- [11] H. Chung, A. Ioinovici, and S. Member, '*Design of Feedback Gain Vector of Two-State Basic PWM Multifeedback Regulators for Large-Signal Stability*', Vol. 44, N°8, pp. 676 - 683, 1997.
- [12] I.M. Pop-Calimanu and F. Renken, '*New multiphase hybrid boost converter with wide conversion ratio for PV system*', *International Journal of Photoenergy*, Vol. 2014, 16 p., 2014.
- [13] Y. Che, W. Zhang, L. Ge, and J. Zhang, '*A two-stage wind grid inverter with boost converter*', *Journal of Applied Mathematics*, Vol. 2014, Special N°2014, 5 p., 2014.
- [14] B. Allaoua, B. Mebarki, and A. Laoufi, '*Applied on Boost DC-DC Converter Power Supply for Electric Vehicle Propulsion System*', *International Journal of Vehicular Technology*, Vol. 2013, 9 p., 2013.
- [15] J. Moreno-valenzuela and O. García-alarcón, '*On Control of a Boost DC-DC Power Converter under Constrained Input*', *Complexity*, Vol. 2017, N°3, pp. 1 - 11, 2017.
- [16] K. Sundareswaran and V.T. Sreedevi, '*Design and development of feed-back controller for a boost converter using a colony of foraging bees*', *Electric Power Components and Systems*, Vol. 37, N°5, pp. 465 - 477, 2009.
- [17] T.T. Vu, '*Non-linear Dynamic Transformer Modelling and Optimum Control Design of Switched-mode Power Supplies*', National University of Ireland Maynooth, 2014.
- [18] B.-S. Lee, S.-K. Kim, J.-H. Park, and K.-B. Lee, '*Adaptive output voltage tracking controller for uncertain DC/DC boost converter*', *International Journal Electronics*, Vol. 103, N°6, pp. 1002 - 1017, 2016.
- [19] P.C. Sen Alexander, G. Perry, Guang Feng, Yan-Fei Liu, '*A Design Method for PI-like Fuzzy Logic Controllers for DC-DC Converter*', *IEEE Transactions on Industrial Electronics*, Vol. 54, N°5, pp. 2688 - 2696, 2007.
- [20] F.D. Menga, N. Djongyang, D. Raïdandi, and R. Tchinda, '*A proportional integral synthesis for a variable speed wind energy conversion system using permanent magnet synchronous generator*', *African Journal of Science, Technology, Innovation and Developpement*, Vol. 8, N°2, pp. 166 -172, 2016.
- [21] M.M. Shebani, T. Iqbal, and J.E. Quaicoe, '*Modified Droop Method Based on Master Current Control for Parallel-Connected DC-DC Boost Converters*', *Journal of Electrical and Computer Engineering*, Vol. 2018, 14p., 2018.
- [22] Branko L. Dokić and B. Blanuša, '*Power Electronics Converter and Regulator*', Switzerland: Springer International Publishing, 2015.
- [23] R. Shenbagalakshmi and T. Sree Renga Raja, '*Observer based pole placement and linear quadratic optimization for DC-DC converters*', *Journal of Electrical Engineering*, Vol. 12, N°4, pp. 1 - 8, 2012.
- [24] A. Yazdani and R. Iravani, '*Voltage-Sourced Converters in Power Systems: Modeling, Control, and Applications*', John Wiley & Sons, Inc, 2010.
- [25] S. Ang and A. Oliva, '*Power-Switching Converter*', Second Edition, CRC Press, 2005.
- [26] S.J. Ovaska and L.M. Sztandera, Eds., '*Soft Computing in Industrial Electronics*', Springer-Verlag, 2002.

- [27] R. Shenbagalakshmi and T. Sree Renga Raja, '*Modelling and Simulation of Digital Compensation Technique for dc–dc Converter by Pole Placement*', Journal of the Institution of Engineers, Series B, Vol. 96, N°3, pp. 265 - 271, 2015.
- [28] I. Munteanu, A.I. Bratcu, N.-A. Cutululis, and E. Ceanga, '*Optimal control of wind energy systems: towards a global approach*', Springer-Verlag, 2008.
- [29] M. Zhu and F.L. Luo, '*Graphical analytical method for power dc-dc converters: Averaging binary tree structure representation*', IEEE Transactions on Power Electronics, Vol. 22, N°2, pp. 701 - 705, 2007.
- [30] T. Ackermann, Ed., '*Wind Power in Power Systems*', Vol. 8., John Wiley & Sons Ltd, 2005.
- [31] H. Sira-Ramírez and R. Silva-Ortigoza, '*Control Design Techniques in Power Electronics Devices*', Springer-Verlag London, 2006.
- [32] C.H. Houpis and S.N. Sheldon, '*Linear Control System Analysis and Design with Matlab*', Sixth, CRC Press, 2013.
- [33] A.M. Trzynadlowski, Ed., '*Power Electronic Converters and Systems: Frontiers and Applications*', The Institution of Engineering and Technology, 2015.
- [34] A. Tewari, '*Modern Control Design With Matlab and Simulink*', John Wiley & Sons Ltd, 2002.
- [35] D. Xue, Y. Chen, and D.P. Atherton, '*Linear Feedback Control Analysis and Design with Matlab*', SIAM, 2007.
- [36] L.Y. Chang, K.H. Chao, and T.C. Chang, '*Application of high voltage ratio and low ripple interleaved DC-DC converter for a fuel cell*', Scientific World Journal, Vol. 2012, N°1, pp. 26 - 36, 2012.
- [37] Mathworks, '*Control System Toolbox™ Getting Started Guide R2014b*', Mathworks, 2014.
- [38] H. Siraramirez, '*Design of P-I controllers for dc-to-dc power supplies via extended linearization*', International Journal of Control, Vol. 51, N°3, pp. 601 - 620, 1990.
- [39] L. Qingfeng, L. Zhaoxia, S. Jinkun, and W. Huamin, '*A Composite PWM Control Strategy for Boost Converter*', Physics Procedia, Vol. 24, pp. 2053 - 2058, 2012.